

Generalization of spectral bulk–boundary correspondence

Shun Tamura¹, Shintaro Hoshino², and Yukio Tanaka¹

¹*Department of Applied Physics, Nagoya University, Nagoya 464-8603, Japan*

²*Department of Physics, Saitama university, Saitama 338-8570, Japan*

(Dated: December 24, 2024)

The bulk–boundary correspondence in one dimension asserts that the physical quantities defined in the bulk and at the edge are connected, as well established in the argument for electric polarization. Recently, a spectral bulk–boundary correspondence (SBBC), an extended version of the conventional bulk–boundary correspondence to energy-dependent spectral functions, such as Green’s functions, has been proposed in chiral symmetric systems, in which the chiral operator anticommutes with the Hamiltonian. In this study, we extend the SBBC to a system with impurity scattering and dynamical self-energies, regardless of the presence or absence of a gap in the energy spectrum. Moreover, the SBBC is observed to hold even in a system without chiral symmetry, which substantially generalizes its concept. The SBBC is demonstrated with concrete models, such as superconducting nanowires and a normal metallic chain. Its potential applications and certain remaining issues are also discussed.

I. INTRODUCTION

Bulk–boundary correspondence (BBC) plays an important role in topological systems in which the physical quantities defined in the bulk and at the edge are connected. This relation is useful because the physics at the surface can be determined from the bulk, which is theoretically easier to handle. In topological materials, the number of zero-energy states appearing on the surface is predicted by an integer topological number, such as a Chern number or winding number defined in the bulk [1–7]. The topological number is immune to a perturbation that does not break the symmetry of a Hamiltonian, and its value can be changed only through a topological quantum phase transition. In addition, the BBC is known in the physics of electric polarization: the amount of accumulated charge is predicted by a geometric Berry phase defined in the bulk [8–10]. In contrast to the topological number, the electric polarization changes its value by perturbation, but the BBC still holds.

In chiral symmetric systems, where the Hamiltonian H anticommutes with a chiral operator Γ , as $H\Gamma + \Gamma H = 0$, a topological number called a winding number W can be defined. It is related to the number of edge modes. In our previous paper [11], we reported that the BBC for chiral symmetric systems can be extended to a nonzero frequency ω , where the complex number of $W(\omega)$ is identical to a spectral function (i.e., Green’s function) integrated over the edge region. We refer to this relation as a spectral bulk–boundary correspondence (SBBC). The SBBC was proved by Daido and Yanase [12], by utilizing an analogy to the concept of electric polarization. We also indicated that, for superconductors with chiral symmetry, an odd-frequency Cooper pair [13–15], which is characterized by a pair amplitude with an odd function in time or frequency, is induced at the surface and is related to the Green’s functions defined in the bulk. The SBBC has been demonstrated for mean-field systems, which are described as one-body Hamiltonians without retardation effects included in the self-energies. Moreover, the impu-

rity effect in the bulk has not been considered; however, it needs to be considered when comparing the results with those of real materials in which disorders are always present.

In this paper, we discuss the generalization of the SBBC. We demonstrate that the SBBC holds for any amplitude of impurity in the bulk, after averaging the physical quantities over the impurity configurations. The effect of the frequency-dependent self-energy that can appear due to tunneling [16] is also considered, where the SBBC still holds. We further demonstrate that the SBBC can be applied to non-chiral-symmetric systems. More specifically, although the existence of the chiral operator is necessary, it does not necessarily anticommute with the Hamiltonian for the SBBC. We also provide an outline of the proof for the generalized SBBC, along with the proof provided in Ref. [12].

The remainder of this paper is organized as follows. In Sec. II, we review the SBBC established in previous studies. In Sec. III, we show how the SBBC is generalized and demonstrate it with several models. We highlight the possible applications of the SBBC in Sec. IV, and summarize our results in Sec. V.

II. SPECTRAL BULK–BOUNDARY CORRESPONDENCE

This section briefly reviews the SBBC established in previous studies [11, 12]. For topological systems, there is a relation between a topological number, which is defined in the bulk, and the number of zero-energy edge modes appearing at the edge of a semi-infinite system. This nontrivial correspondence can be extended to a nonzero frequency for chiral symmetric systems.

For one-dimensional systems with chiral symmetry without many-body interaction, we can denote the

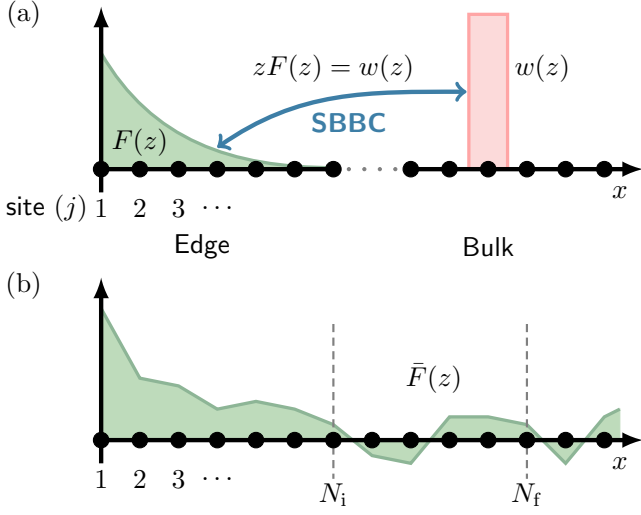


FIG. 1. Schematic illustration of (a) SBBC and (b) $\bar{F}(z)$

Hamiltonian for a semi-infinite system as

$$\hat{H} = \sum_{i,j>0} \Psi_i^\dagger H_{i,j} \Psi_j, \quad (1)$$

with $\Psi_i = (c_{i,1}, \dots, c_{i,m})$ where $c_{i,\alpha}$ ($\alpha = 1, \dots, m$) is the annihilation operator for the i -th unit cell, and α indicates an index of the internal degree of freedom, such as a spin or orbital. In this study, we set the lattice constant as a unit of length. Equation (1) is used to calculate the physical quantities at the edge. In contrast, the bulk quantities are calculated in the Hamiltonian with the periodic boundary condition given by

$$\hat{h} = \sum_k \psi_k^\dagger h(k) \psi_k, \quad (2)$$

with $\psi_k = (c_{k,1}, \dots, c_{k,m})$ where $c_{k,\alpha}$ ($\alpha = 1, \dots, m$) is the annihilation operator for the momentum k . Here, $H_{i,j}$ and $h(k)$ anticommute with $m \times m$ chiral operators Γ , where the relation $\{H_{i,j}, \Gamma\} = \{h(k), \Gamma\} = 0$ is satisfied with $\text{Tr}\Gamma=0$ [17]. To avoid confusion, we use upper-case letters to denote the physical quantities in a semi-infinite system with a boundary at $j = 0$, and lower-case letters to denote those in a periodic system designed for the bulk (see Appendix A).

Then, the SBBC is explicitly written as

$$zF(z) = w(z), \quad (3)$$

with

$$F(z) = \sum_{j>0} \text{Tr}[\Gamma G_{j,j}(z)], \quad (4)$$

$$w(z) = \frac{1}{2iN_{\text{unit}}} \sum_k \text{Tr}[\Gamma g(k, z) \partial_k g^{-1}(k, z)], \quad (5)$$

where N_{unit} is the number of unit cells with sufficiently large values for convergence. The trace Tr is taken in

an $m \times m$ space. Here, $G_{i,j}(z)$ and $g(k, z)$ are Green's functions given by $G_{i,j}(z) = (z - H)_{i,j}^{-1}$ and $g(k, z) = [z - h(k)]^{-1}$, respectively, where z is a complex number that can be regarded as a generalized frequency. Notably, $F(z)$ is an odd function of z given by

$$\begin{aligned} F(z) &= \sum_{j>0} \text{Tr}[\Gamma(z - H)_{j,j}^{-1}] \\ &= \sum_{j>0} \text{Tr}[(z + H)_{j,j}^{-1} \Gamma] \\ &= -F(-z). \end{aligned} \quad (6)$$

Then, $F(z)$ is given by the spatial sum of odd-frequency correlation functions in the edge region. For superconductors, $F(z)$ can be the sum of anomalous Green's functions, and it is regarded as an odd-frequency Cooper pair amplitude [13–15]. A schematic of the SBBC is shown in Fig. 1(a). Note that, in the limit $z \rightarrow 0$ in Eq. (3), $zF(z)$ and $w(z)$ become

$$\lim_{z \rightarrow 0} zF(z) = \lim_{z \rightarrow 0} w(z) = W, \quad (7)$$

where W is an integer winding number [5, 18], and Eq. (7) is a conventional bulk–boundary correspondence [19]. Notably, W can be well defined only when an energy gap at zero energy is opened. From Eq. (7), the SBBC is regarded as an extension of the conventional bulk–boundary correspondence at zero frequency to a nonzero frequency.

Note that Eq. (5) can be rewritten in real space by applying a Fourier transformation as follows:

$$w(z) = \frac{1}{2iN_{\text{unit}}} \bar{\text{Tr}} \{ \bar{\Gamma} g(z) i[g^{-1}(z), \bar{x}] \}, \quad (8)$$

with

$$g_{i,j}(z) = \frac{1}{N_{\text{unit}}} \sum_k g(k, z) e^{ik(r_i - r_j)}, \quad (9)$$

$$h_{i,j} = \frac{1}{N_{\text{unit}}} \sum_k h(k) e^{ik(r_i - r_j)}, \quad (10)$$

$$\bar{\Gamma}_{i,j} = \Gamma \delta_{i,j}, \quad (11)$$

where r_i is a spatial coordinate of the unit cell, and the trace $\bar{\text{Tr}}$ is taken for an $mN_{\text{unit}} \times mN_{\text{unit}}$ matrix. Note that we have used the same symbol g for both the real space and the k -space, and the symbols are distinguished by explicitly writing the arguments in parentheses. \bar{x} is a *position operator* defined by

$$\bar{x} = \text{diag}(r_1 I_m, r_2 I_m, \dots, r_{N_{\text{unit}}} I_m), \quad (12)$$

where I_m is an $m \times m$ identity matrix [20–22]. As discussed in the following section, this real-space representation is crucial when we discuss the SBBC in the presence of impurities in the bulk, where the wavenumber is no longer a good quantum number unless we take the average over the impurity configuration.

III. GENERALIZED SBBC

The SBBC can be applied to a system with impurities in the bulk and to a system without chiral symmetry, by changing its formula. In Sec. III A, we provide a generalized version of the SBBC. From Sec. III B to III D, several examples of superconducting and nonsuperconducting systems in one dimension are studied. In Sec. III B, we discuss a Kitaev chain with impurities in which chiral symmetry is preserved. In Sec. III C, we discuss the self-energy effect on a Rashba nanowire proximately coupled to an s -wave superconductor. In Sec. III D, a Schrieffer–Heeger (SSH) model with chemical potential, which breaks the chiral symmetry, is discussed.

A. Reformulation of SBBC

This subsection considers a large but finite system with N_{unit} unit cells instead of a semi-infinite system. We reformulate Eqs. (4) and (5) for a system with impurities and self-energy. First, we define the quantities at the boundary as follows:

$$\bar{F}(z) = \langle F_j(z) \rangle_j, \quad (13)$$

$$F_j(z) = \sum_{l=1}^j \bar{\text{Tr}} \{ \mathcal{N}_l \bar{\Gamma} [1 - \Sigma_c(z)/z] \bar{G}(z) \}, \quad (14)$$

$$\bar{G}(z) = [z - H - \Sigma_c(z) - \Sigma_{\text{ac}}(z)]^{-1}, \quad (15)$$

where

$$0 = \{ \bar{\Gamma}, H \} = [\bar{\Gamma}, \Sigma_c(z)] = \{ \bar{\Gamma}, \Sigma_{\text{ac}}(z) \}, \quad (16)$$

and $\langle \dots \rangle_j = \frac{1}{N_f - N_i + 1} \sum_{j=N_i}^{N_f} [\dots]$, which performs self-averaging on the randomness of the impurity potentials [23]. We choose N_i and N_f far from both edges [see Fig. 1(b) for a schematic], and we assume that $N_f - N_i$ is sufficiently large. In addition, \mathcal{N}_l is introduced by $(\mathcal{N}_l)_{i,j} = I_m \delta_{i,l} \delta_{j,l}$. Here, the suffixes “c” and “ac” indicate the commuting and anticommuting parts of the self-energy with the chiral operator, respectively. Notably, any $2^n \times 2^n$ (integer n) matrix can be decomposed by the products of the Pauli matrix, and any $2^n \times 2^n$ matrix can be decomposed into commutable and anti-commutable parts, as in Eq. (16) [24].

Here, the self-energy $\Sigma(z) \equiv \Sigma_c(z) + \Sigma_{\text{ac}}(z)$, which is divided into two parts, may be regarded as a part of the Hamiltonian if the z -dependence is absent. In general, the presence of self-energy invalidates the chiral symmetry, which is defined as $\{ \bar{\Gamma}, H + \Sigma \} = 0$, or equivalently, $\Sigma_c(z) = 0$. Nevertheless, the SBBC generally holds, as shown in the following section.

From the definition of $\bar{F}(z)$ in Eq. (13), the summation $\sum_{j=N_i}^{N_f}$ takes an average far from the edge and provides a mean value of $F_j(z)$ in the range $F_{N_i}(z)$ to $F_{N_f}(z)$ [Fig. 1(b)]. If there is translational symmetry far from both edges, $F_j(z)$ is independent of j , as it is determined

by the bulk properties. In the limit $N_{\text{unit}} \rightarrow \infty$ with $N_f - N_i \rightarrow \infty$ while keeping N_i and N_f sufficiently far from both edges, it can be expected that $z\bar{F}(z)$ converges to some value.

Next, we consider the quantities in the bulk. The procedure is similar to the real-space representation discussed at the end of the previous section, but with the consideration of self-energy. Namely, we define the quantities as

$$\bar{w}(z) = \frac{1}{2iN_{\text{unit}}} \bar{\text{Tr}} \{ \bar{\Gamma} \bar{g}(z) i [\bar{g}^{-1}(z), \bar{x}] \}, \quad (17)$$

$$\bar{g}(z) = [z - h - \sigma_c(z) - \sigma_{\text{ac}}(z)]^{-1}, \quad (18)$$

with

$$0 = \{ \bar{\Gamma}, h \} = [\bar{\Gamma}, \sigma_c(z)] = \{ \bar{\Gamma}, \sigma_{\text{ac}}(z) \}. \quad (19)$$

Note that the translational symmetry is not assumed in these expressions even in the bulk.

With the above definitions, the relation between $\bar{F}(z)$ and $\bar{w}(z)$ is given by

$$z\bar{F}(z) = \bar{w}(z). \quad (20)$$

which is one of the main results of this study. We emphasize that Eq. (3) and Eq. (20) have the same functional form, but the latter can now be applied to non-chiral-symmetric and non-translation-symmetric systems. See also Appendix B for the derivation. Notably, when $\Sigma_c(z) \neq 0$ or $\Sigma_{\text{ac}}(z) \neq 0$, the spectral function $\bar{F}(z)$ in the generalized SBBC can be a mixture of even and odd functions of z . In the following subsections, we will demonstrate several relevant examples.

When there is an impurity potential, we suppose that both the Hamiltonians with the open and periodic boundary conditions contain the impurity with the same impurity amplitude and probability distribution. In Sec. III B and Sec. III D, we use a uniform distribution of random numbers, and adopt $N_i = N_{\text{unit}}/4$ and $N_f = N_{\text{unit}}/2$.

Without an impurity potential, $\bar{w}(z)$ can be written as

$$\bar{w}(z) = \frac{1}{2iN_{\text{unit}}} \sum_k \text{Tr} [\Gamma \bar{g}(k, z) \partial_k \bar{g}^{-1}(k, z)], \quad (21)$$

where $\bar{g}(k, z)$ is obtained by applying Fourier transformation to $\bar{g}(z)$. This recovers the original SBBC discussed in the previous section. Notably, if $\sigma_c(z) = 0$, $\bar{w}(z = 0)$ is an integer as long as the spectral gap remains open.

B. Kitaev chain with impurity

We numerically demonstrate the impurity effect on the SBBC for a Kitaev chain [25], which is a model for a spin-polarized one-dimensional p -wave superconductor. This model possesses chiral symmetry, and the Hamiltonian is

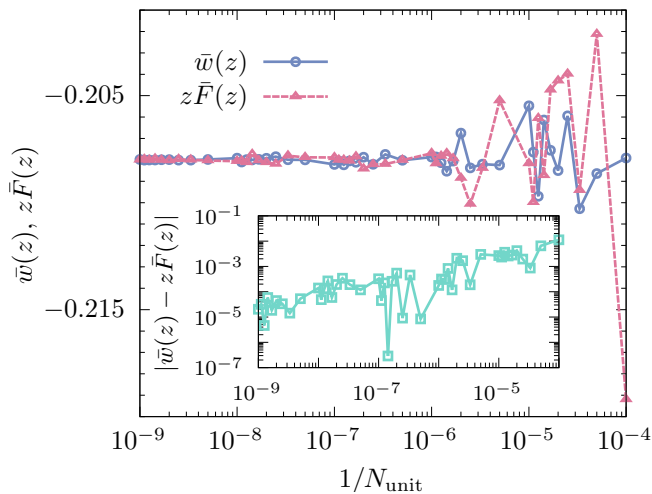


FIG. 2. $\bar{w}(z)$ and $z\bar{F}(z)$ plotted as a function of $1/N_{\text{unit}}$ for $\mu/t = 0$, $\Delta/t = 0.1$, $z/t = 0.1i$, and $V_\mu = 2$. $|\bar{w}(z) - z\bar{F}(z)|$ shown as a function of $1/N_{\text{unit}}$ in the inset

given by

$$\mathcal{H} = -t \sum_j \left(c_j^\dagger c_{j+1} + \text{H.c.} \right) + \sum_j [\mu + t f_\mu(j)] c_j^\dagger c_j + \Delta \sum_j \left(c_j^\dagger c_{j+1}^\dagger + \text{H.c.} \right), \quad (22)$$

where c_j (c_j^\dagger) is the annihilation (creation) operator for the j -th site, t is the hopping integral, μ is the chemical potential, Δ is the superconducting pair potential, and $f_\mu(j)$ is the impurity potential with $|f_\mu(j)| < V_\mu$. The chiral operator is given by $\Gamma = \sigma_1$ with the Pauli matrix σ_1 in the particle-hole space. To calculate $\bar{w}(z)$ and $\bar{F}(z)$, we use a recursive Green's function method [26] with the matrix transformation technique [27], which enables us to access a large system.

In Fig. 2, $\bar{w}(z)$ and $z\bar{F}(z)$ are shown as a function of the inverse of N_{unit} to examine the system size dependence. Notably, we do not take a sample average, but prepare only one sample. This graph shows that, with an increase in N_{unit} , $\bar{w}(z)$ and $z\bar{F}(z)$ converge to the same value. The difference between $z\bar{F}(z)$ and $\bar{w}(z)$ is also plotted in the inset of Fig. 2, and it decreases as N_{unit} increases.

Even in the presence of an impurity potential, the winding number W can be defined when an energy gap is opened [28]. On the other hand, $\bar{w}(z)$ and $\bar{F}(z)$ are always well defined as long as z is not equal to the eigenvalues of the Hamiltonian (which is avoided on the Matsubara axis), regardless of the presence or absence of an energy gap in the spectrum.

C. Rashba nanowire

In this subsection, we consider a Green's function with self-energy for a Rashba nanowire system [29–31]. The

Rashba nanowire system has attracted considerable attention because it hosts Majorana fermions at both edges. Figure 3 illustrates a Rashba nanowire system that possesses a large Rashba spin-orbit interaction and is proximately coupled to an s -wave superconductor. The Hamiltonian for the Rashba nanowire system is

$$\mathcal{H}_{\text{RN}} = -t \sum_{j,\sigma} \left(c_{j,\sigma}^\dagger c_{j+1,\sigma} + \text{H.c.} \right) - \mu \sum_{j,\sigma} c_{j,\sigma}^\dagger c_{j,\sigma} + B \sum_{j,\sigma,\sigma'} c_{j,\sigma}^\dagger (\hat{\sigma}_3)_{\sigma,\sigma'} c_{j,\sigma'} + \frac{i\alpha}{2} \sum_{j,\sigma,\sigma'} \left[c_{j,\sigma}^\dagger (\hat{\sigma}_2)_{\sigma,\sigma'} c_{j+1,\sigma'} - \text{H.c.} \right], \quad (23)$$

with a Pauli matrix $\hat{\sigma}_i$ ($i = 1, 2, 3$) in the spin space. Here, B is the magnetic field, and α is the Rashba spin-orbit interaction. The s -wave pair potential is included in the self-energy [16] and is given by

$$\Sigma(i\omega_n) = -|\tilde{t}|^2 \nu_{\text{F}} \left[\frac{\omega_n + \Delta_s \hat{\sigma}_2 \hat{\tau}_2}{\sqrt{\Delta_s^2 - \omega_n^2}} + \zeta \hat{\tau}_3 \right], \quad (24)$$

where \tilde{t} is the hopping between the nanowire and the superconductor, ν_{F} is the density of states (DOS) at the surface of the superconductor at the Fermi energy, ω_n is the Matsubara frequency, Δ_s is the s -wave pair potential of the superconductor, ζ is the proximity-induced chemical potential shift, and $\hat{\tau}_i$ ($i = 1, 2, 3$) is a Pauli matrix in the particle-hole space. Namely, the retardation effect associated with electron tunneling between the nanowire and the superconductor is expressed as the frequency-dependent self-energy.

The chiral operator in Eq. (23) is $\Gamma = \hat{\tau}_1$, and the self-energy in Eq. (24) can be decomposed as $\Sigma(i\omega_n) = \Sigma_c(i\omega_n) + \Sigma_{\text{ac}}(i\omega_n)$ with

$$\Sigma_c(i\omega_n) = -|\tilde{t}|^2 \nu_{\text{F}} \frac{\omega_n}{\sqrt{\Delta_s^2 - \omega_n^2}}, \quad (25)$$

$$\Sigma_{\text{ac}}(i\omega_n) = -|\tilde{t}|^2 \nu_{\text{F}} \left[\frac{\Delta_s \hat{\sigma}_2 \hat{\tau}_2}{\sqrt{\Delta_s^2 - \omega_n^2}} + \zeta \hat{\tau}_3 \right]. \quad (26)$$

For the open boundary system, self-energy can have site dependence close to the surface, although it is independent of the site for the bulk. As discussed in Refs. [11, 12], $\bar{F}(z)$ does not change its value with the surface modulation of the Hamiltonian or the self-energy. Therefore, we can use the value of the self-energy in the bulk, even at the boundary. From the above Hamiltonian and self-energy, we can explicitly write the SBBC relation (20).

When the direction of the magnetic field is perpendicular to the Rashba spin-orbit interaction, the Hamiltonian Eq. (23) has chiral symmetry, and there are Majorana fermions at both edges in a topological phase. Notably, when their directions are not perpendicular to each other, these Majorana fermions are still present up to a certain angle [32], and the SBBC also holds.

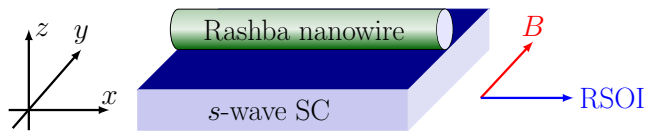


FIG. 3. Schematic of normal metal Rashba nanowire on s -wave superconductor (SC); RSOI represents Rashba spin-orbit interaction.

D. DOS and SBBC for SSH model

1. Without impurity

The concept of SBBC can also be applied to nonsuperconducting systems. In this subsection, we first discuss the relationship between $F(z)$ and the DOS for an SSH model with chiral symmetry, which is a model for polyacetylene [33, 34]. Then, we discuss the SBBC for an SSH model with a nonzero value of chemical potential, which breaks the chiral symmetry.

The SSH model has two sublattices in the unit cell. The Hamiltonian is given by

$$\begin{aligned} \mathcal{H}_{\text{SSH}} = & -t_1 \sum_j \left(c_{j,A}^\dagger c_{j,B} + \text{H.c.} \right) \\ & - t_2 \sum_j \left(c_{j,B}^\dagger c_{j+1,A} + \text{H.c.} \right) \end{aligned} \quad (27)$$

$$= \sum_k \begin{pmatrix} c_{k,A}^\dagger & c_{k,B}^\dagger \end{pmatrix} h(k) \begin{pmatrix} c_{k,A} \\ c_{k,B} \end{pmatrix}, \quad (28)$$

$$h(k) = [-(t_1 + t_2 \cos k)\tau_1 - t_2 \sin k\tau_2], \quad (29)$$

where A and B denote the sublattices, and τ_j with $j = 1, 2, 3$ is a Pauli matrix in the sublattice space. Here, the chiral operator is $\Gamma = \tau_3$, and only the diagonal elements of the chiral operator are nonzero. The SSH model becomes topologically nontrivial when $t_2/t_1 > 1$, as characterized by the nonzero winding number.

From the SBBC with $z = i\omega_n$, $F(i\omega_n)$ is related to an odd-frequency charge density wave as follows [35]:

$$F(i\omega_n) = \int_0^\beta d\tau e^{i\omega_n \tau} \sum_{j>0} \langle c_{j,A}^\dagger(\tau) c_{j,A}(0) - c_{j,B}^\dagger(\tau) c_{j,B}(0) \rangle. \quad (30)$$

Through the analytic continuation, $F(z = E + i\eta)$ with a positive infinitesimal η is related to the difference in the DOS between the A and B sublattices because the local DOS is given by the imaginary part of the retarded Green's function, $\rho(E, j) = -\frac{1}{\pi} \text{Im} G_{j,j}(z = E + i\eta)$:

$$-\frac{1}{\pi} \text{Im} F(E + i\eta) = \rho_A(E) - \rho_B(E). \quad (31)$$

Here, $\rho_{A(B)}$ is the DOS at the A(B) sublattice given by $\rho_{A(B)}(E) = -\frac{1}{\pi} \text{Im} \sum_j G_{(j,A(B)),(j,A(B))}(E + i\eta)$. Equa-

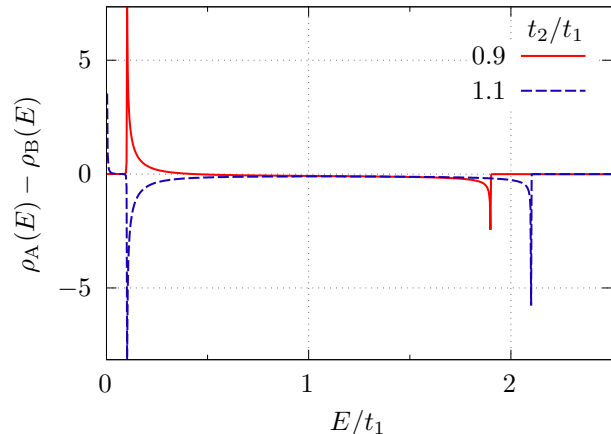


FIG. 4. Difference in the local DOS plotted as a function of E for $t_2/t_1 = 0.9$ (topologically trivial) and 1.1 (topologically nontrivial)

tion (31) can be derived from $\Gamma = \tau_3$ as follows:

$$F(z) = \sum_{j>0} [G_{(j,A),(j,A)}(z) - G_{(j,B),(j,B)}(z)]. \quad (32)$$

Then, from the SBBC, the difference in the DOS between the A and B sublattices for the semi-infinite system can be predicted from the bulk value $w(E + i\eta)$ (see Appendix C). Figure 4 shows $\rho_A(E) - \rho_B(E)$. In the topologically nontrivial phase, $\rho_A(E) - \rho_B(E)$ diverges at $E = 0$ (Fig. 4 with $t_2/t_1 = 1.1$). For superconductors, $F(z)$ is related to an anomalous Green's function and is difficult to detect because the anomalous Green's function is a gauge-dependent quantity. Conversely, $F(z)$ for the SSH model is composed of a normal Green's function, which can be measured.

In Eqs. (27), (28), and (29), the chemical potentials are set to zero, and the Hamiltonian has chiral symmetry, that is, it anticommutes with the chiral operator. On the other hand, in a more realistic situation, the chemical potentials are not zero.

$$\mathcal{H} = \mathcal{H}_{\text{SSH}} - \mu_A \sum_j n_{j,A} - \mu_B \sum_j n_{j,B}, \quad (33)$$

with $n_{j,A(B)} = c_{j,A(B)}^\dagger c_{j,A(B)}$. In this case, \mathcal{H} does not have chiral symmetry, but the SBBC holds. We can choose any $\tau_{i=1,2,3}$ for Γ , indicating that there are several SBBC relations for a given physical system. More generally, we can choose the superposition of these Pauli matrices in principle (see Sec. IV). When we choose $\Gamma = \tau_3$,

$$\Sigma_c(z) = -\mu_A \sum_j n_{j,A} - \mu_B \sum_j n_{j,B}, \quad (34)$$

$$\sigma_c(z) = -\mu_A(\tau_0 + \tau_3)/2 - \mu_B(\tau_0 - \tau_3)/2. \quad (35)$$

Notably, the extended version of the winding number $\bar{w}(z)$ with $z = 0$ is not an integer for the nonzero value

of μ_A or μ_B . Then, $\bar{F}(z)$ is

$$\begin{aligned} \bar{F}(z) &= \sum_{j=1}^{N_f} [\bar{G}_{(j,A),(j,A)}(z) - \bar{G}_{(j,B),(j,B)}(z)] \\ &+ \frac{1}{z} \sum_{j=1}^{N_f} [\mu_A \bar{G}_{(j,A),(j,A)}(z) - \mu_B \bar{G}_{(j,B),(j,B)}(z)]. \end{aligned} \quad (36)$$

A comparison between Eq. (32) and Eq. (36) indicates that $\bar{F}(z)$ has an additional term. On the other hand, for $\Gamma = \tau_1$ or τ_2 , $\bar{F}(z)$ contains off-diagonal elements of the Green's function, and it is difficult to obtain a concise physical interpretation. Notably, the SSH model with chemical potential can be metallic, and the SBBC still holds.

2. With impurity

In Sec. III B, the Kitaev chain with an impurity, which does not break the chiral symmetry, is considered. Here, we consider the SBBC for the SSH model with an on-site impurity potential, which breaks the chiral symmetry [36]. The Hamiltonian is given by

$$\begin{aligned} \mathcal{H}_{\text{SSH}}^{\text{imp.}} &= \mathcal{H}_{\text{SSH}} - \sum_j [\mu_A + t_1 f_{\mu_A}(j)] n_{j,A} \\ &- \sum_j [\mu_B + t_1 f_{\mu_B}(j)] n_{j,B}. \end{aligned} \quad (37)$$

Here, $f_{\mu_{A(B)}}$ is a random number that satisfies $|f_{\mu_{A(B)}}| < V_{\mu_{A(B)}}$. In Fig. 5, $\bar{w}(z)$ and $z\bar{F}(z)$ are shown as a function of N_{unit} . $\bar{w}(z)$ and $z\bar{F}(z)$ converge to the same value, and the difference between them becomes smaller as N_{unit} increases, as shown in the inset of Fig. 5. Although the proof given in Appendix B has already provided firm evidence for the correspondence between the bulk and the edge, the system size dependence is not encoded in the proof. Thus, numerical measurements are necessary, and they provide a quantitative estimate of the system size when the SBBC is applicable.

IV. DISCUSSION

Here, we discuss the possible applications of the SBBC. As demonstrated in this study, the concept of SBBC can be widely used for a one-dimensional structure with correlation functions and is not restricted to chiral symmetric systems, a bulk with translational symmetry, or superconducting systems. The essential aspects for applying the SBBC are to recognize the one-dimensional structure and divide the correlation function matrix into the commuting and anticommuting parts with a chiral operator (see Appendix B). For an illustration from a general

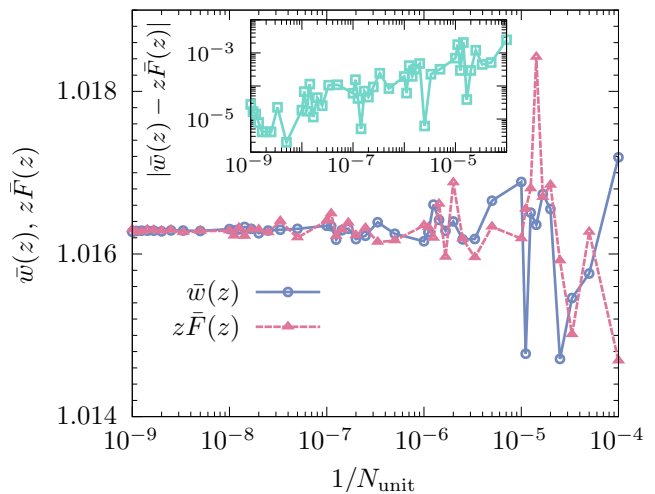


FIG. 5. $\bar{w}(z)$ and $z\bar{F}(z)$ plotted as a function of $1/N_{\text{unit}}$ for $t_2/t_1 = 1.5$, $\mu_A/t_1 = 0.1$, $\mu_B/t_1 = 0.2$, $z/t = 0.1i$, $V_{\mu_A} = 0.5$, and $V_{\mu_B} = 0.8$. $|\bar{w}(z) - z\bar{F}(z)|$ shown as a function of $1/N_{\text{unit}}$ in the inset

perspective, we consider the single-particle function in equilibrium as follows:

$$G(\sigma, \mathbf{R}_i, \tau_1; \sigma', \mathbf{R}_j, \tau_2) = -\langle \mathcal{T} c_{i\sigma}(\tau_1) c_{j\sigma'}^\dagger(\tau_2) \rangle, \quad (38)$$

where the index i represents the three-dimensional spatial coordinate \mathbf{R}_i of the lattice sites where the electrons are located. We introduce the Heisenberg picture $A(\tau) = e^{\tau H} A e^{-\tau H}$ with imaginary time, and \mathcal{T} is a time-ordering operator. This correlation function should be considered for almost all the electronic systems of interest. For example, it can be calculated through first-principles calculations used to obtain electronic band structures.

Based on this example, we show that there can be, in principle, an infinite number of SBBC relations. For simplicity, we assume that the bulk system has a translational symmetry. First, we define the edge where the surface is perpendicular to the vector \mathbf{k}_\perp . Then, we introduce vectors parallel to the surface \mathbf{k}_\parallel that satisfy $\mathbf{k}_\perp \cdot \mathbf{k}_\parallel = 0$. Similarly, in the spin space, we determine the chiral operator by choosing one of the directions $\boldsymbol{\theta}$, which is a unit vector specifying the direction of the spin, as

$$\Gamma = \boldsymbol{\theta} \cdot \boldsymbol{\sigma}. \quad (39)$$

After the Fourier transformation, the bulk Green's function is written in a matrix form in the spin space as

$$\bar{g}^{-1}(\mathbf{k}_\perp; \mathbf{k}_\parallel, i\omega_n, \boldsymbol{\theta}) = v + \alpha\Gamma + \boldsymbol{\beta} \cdot \boldsymbol{\sigma}, \quad (40)$$

where $\boldsymbol{\theta} \cdot \boldsymbol{\beta} = 0$. From this expression, we can identify the commuting ($v + \alpha\Gamma$) and anticommuting ($\boldsymbol{\beta} \cdot \boldsymbol{\sigma}$) parts with the chiral operator. The vector $\mathbf{h} = \alpha\boldsymbol{\theta} + \boldsymbol{\beta}$ can be regarded as a pseudomagnetic field in the k -space. Note that the scalars v, α and the vector $\boldsymbol{\beta}$ are uniquely

determined from the information of the system once $\boldsymbol{\theta}$ is specified. Based on these expressions, we can express the bulk quantity as follows:

$$\bar{w} = \int \frac{dk_{\perp}}{4\pi i} \text{Tr} (\Gamma \bar{g} \partial_{\perp} \bar{g}^{-1}) \quad (41)$$

$$= \boldsymbol{\theta} \cdot \int \frac{dk_{\perp}}{2\pi i} \frac{v \partial_{\perp} \mathbf{h} - \mathbf{h} \partial_{\perp} v - i \mathbf{h} \times \partial_{\perp} \mathbf{h}}{v^2 - \mathbf{h}^2} \quad (42)$$

$$= \int \frac{dk_{\perp}}{2\pi i} \frac{v \partial_{\perp} \alpha - \alpha \partial_{\perp} v - i \boldsymbol{\theta} \cdot (\boldsymbol{\beta} \times \partial_{\perp} \boldsymbol{\beta})}{v^2 - \alpha^2 - \boldsymbol{\beta}^2}, \quad (43)$$

with $\partial_{\perp} = \frac{\partial}{\partial k_{\perp}}$. Namely, the relations of the BBC are constructed for the *infinite* set of $(\mathbf{k}_{\parallel}, \omega_n, \boldsymbol{\theta})$, although the counterpart quantity at the edge is not necessarily physically interpreted easily if the commuting part has a complicated structure, as shown in Eq. (14). The integrand of Eq. (41) resembles an SU(2) spin-gauge field given by Eqs. (155,156) of Ref. [37], although Eq. (41) is defined in the reciprocal space. The appearance of the gauge-field-like structure is reminiscent of the relationship between the electromagnetic U(1) gauge field (i.e., scalar and vector potentials) and the Berry connection in the \mathbf{k} -space associated with the Bloch wave function [38].

Thus, the appearance of the vector $\boldsymbol{\theta}$ in the spin space and the wave vector $\mathbf{k}_{\perp, \parallel}$ in the real (or reciprocal) space indicates that the SBBC is controlled by spin-orbit coupling. Without complications in the spin and orbital spaces, the SBBC would provide a trivial relation of “0 = 0” between the bulk and the edge. Hence, it is interesting to study a system with various types of spin-orbital couplings in detail, optionally combined with band-structure calculations.

For a system with a gap in the energy spectrum, the correlation length exhibits an exponential decay, which defines the spatially localized edge state well. On the other hand, if we deal with the metallic state, the correlation functions generally decay with a power-law behavior, and the localized state at the edge is ill defined. However, even in this case, the SBBC can be used if the spatial integral from the edge to the bulk converges. For example, this point can be confirmed for the parameters at the topological critical point, where the correlation length diverges.

In the above discussion, we emphasize that we only invoke the presence of the edge and do not use any specific details of the system. For the definition of the edge, the necessary condition is that the original Hamiltonian is composed of link variables with a finite range or decreasing amplitude when the distance increases. This is a generic condition satisfied in most materials. In addition, the extensions to the multiple degrees of freedom inside the unit cell, to the pairing states, and to two-particle correlation functions, such as charge and spin structure factors, are interesting and should be straightforward. Furthermore, the expectation value in Eq. (38) can be evaluated with many-body wave functions and are not restricted to one-body problems. Thus, the SBBC should

be widely applicable to general correlation functions, and it should be applied to extract nontrivial information at the edge from the bulk quantities.

V. SUMMARY AND OUTLOOK

In summary, we established the generalization of the SBBC, which is an extended version of the bulk-boundary correspondence for topological systems. We demonstrated the SBBC through several applications as follows. (i) The SBBC holds for the Kitaev chain with impurities in the bulk, where the Hamiltonian has chiral symmetry. (ii) In principle, the SBBC can be experimentally confirmed for the SSH model using the local DOS. (iii) The SBBC holds for the SSH model with a chemical potential, which breaks the chiral symmetry. (iv) The SBBC holds even if self-energy is included.

We suggest a possible application to a general correlation function in Sec. IV; however, several interesting problems remain. (1) The SBBC is only demonstrated for a one-dimensional system. Whether a similar demonstration is possible for a higher-dimensional system remains to be investigated. (2) When $\sigma_c(z) = 0$ in Eq. (17), $\lim_{z \rightarrow 0} \bar{w}(z)$ is an integer. The relationship between this integer and the number of edge modes for many-body interaction systems remains unexplored. (3) In this study, we adopted Eq. (8) and Eq. (17) as an extended version of the winding number in a real-space representation. Recently, another representation of the winding number related to the Bott index has been suggested [39]. Its possible extension to a nonzero frequency is an interesting problem to be investigated. (4) We only consider $\bar{G}(z)$ in Eq. (15) as the Green’s function. On the other hand, it can be regarded as a general matrix, such as a spin-spin correlation function. This is also an interesting issue.

Thus, the present study presented a general framework for bulk-boundary correspondence. Numerous target systems in which the concept of the SBBC is applicable exist, and they remain to be explored using mathematical and computational techniques.

ACKNOWLEDGMENTS

We are grateful to A. Daido, S. Richard, C. Bourne, M. Lein and H. Katsura for useful discussions. This work was supported by Grant-in-Aid for Scientific Research B (KAKENHI Grant No. JP18H01176 and No. JP20H01857) from the Ministry of Education, Culture, Sports, Science, and Technology, Japan (MEXT) and Grant-in-Aid for Scientific Research A (KAKENHI Grant No. JP20H00131), the JSPS Core-to-Core program Oxide Superspin International Network and Researcher Exchange Program between JSPS and RFBR (JPJSBP120194816). This work was also supported by Japan Society for Promotion of Science (JSPS) KAKENHI Grant No. 18K13490.

- [1] D. J. Thouless, M. Kohmoto, M. P. Nightingale, and M. den Nijs, Quantized hall conductance in a two-dimensional periodic potential, *Phys. Rev. Lett.* **49**, 405 (1982).
- [2] M. Kohmoto, Topological invariant and the quantization of the hall conductance, *Annals of Physics* **160**, 343 (1985).
- [3] S. Ryu and Y. Hatsugai, Topological origin of zero-energy edge states in particle-hole symmetric systems, *Phys. Rev. Lett.* **89**, 077002 (2002).
- [4] M. Z. Hasan and C. L. Kane, Colloquium: Topological insulators, *Rev. Mod. Phys.* **82**, 3045 (2010).
- [5] M. Sato, Y. Tanaka, K. Yada, and T. Yokoyama, Topology of andreev bound states with flat dispersion, *Phys. Rev. B* **83**, 224511 (2011).
- [6] X.-L. Qi and S.-C. Zhang, Topological insulators and superconductors, *Rev. Mod. Phys.* **83**, 1057 (2011).
- [7] C.-K. Chiu, J. C. Y. Teo, A. P. Schnyder, and S. Ryu, Classification of topological quantum matter with symmetries, *Rev. Mod. Phys.* **88**, 035005 (2016).
- [8] R. D. King-Smith and D. Vanderbilt, Theory of polarization of crystalline solids, *Phys. Rev. B* **47**, 1651 (1993).
- [9] D. Vanderbilt and R. D. King-Smith, Electric polarization as a bulk quantity and its relation to surface charge, *Phys. Rev. B* **48**, 4442 (1993).
- [10] R. Resta, Macroscopic polarization in crystalline dielectrics: the geometric phase approach, *Rev. Mod. Phys.* **66**, 899 (1994).
- [11] S. Tamura, S. Hoshino, and Y. Tanaka, Odd-frequency pairs in chiral symmetric systems: Spectral bulk-boundary correspondence and topological criticality, *Phys. Rev. B* **99**, 184512 (2019).
- [12] A. Daido and Y. Yanase, Chirality polarizations and spectral bulk-boundary correspondence, *Phys. Rev. B* **100**, 174512 (2019).
- [13] Y. Tanaka, M. Sato, and N. Nagaosa, Symmetry and topology in superconductors –odd-frequency pairing and edge states–, *Journal of the Physical Society of Japan* **81**, 011013 (2012).
- [14] J. Linder and A. V. Balatsky, Odd-frequency superconductivity, *Rev. Mod. Phys.* **91**, 045005 (2019).
- [15] J. Cayao, C. Triola, and A. M. Black-Schaffer, Odd-frequency superconducting pairing in one-dimensional systems, *The European Physical Journal Special Topics* **229**, 545 (2020).
- [16] T. Stanescu and S. Tewari, Majorana fermions in semiconductor nanowires: fundamentals, modeling, and experiment, *Journal of physics. Condensed matter : an Institute of Physics journal* **25**, 233201 (2013).
- [17] $\text{Tr}\Gamma = 0$ is always satisfied when the eigenvalues of the Hamiltonian does not include zero.
- [18] $\Gamma^\dagger = \Gamma$ and $\Gamma^2 = 1$ are necessary to obtain integer W . On the other hand, Eq. (3) holds without these conditions.
- [19] V. Gurarie, Single-particle green's functions and interacting topological insulators, *Phys. Rev. B* **83**, 085426 (2011).
- [20] In Eq. (8), there appears $r_i - r_j$ from $[g(z), \bar{x}]$ and it is noted that $r_1 - r_{N_{\text{unit}}} = 1$ due to the periodic boundary condition. Then the winding number $w(z=0)$ becomes $w(0) = \frac{1}{2iN_{\text{unit}}}\text{Tr}\{\Gamma h^{-1}[h, \bar{x}]\} \neq \frac{1}{iN_{\text{unit}}}\text{Tr}(\Gamma \bar{x})$. It is also noted that for superconductors, \bar{x} does not have physical meaning.
- [21] I. Mondragon-Shem, T. L. Hughes, J. Song, and E. Prodan, Topological criticality in the chiral-symmetric AIII class at strong disorder, *Phys. Rev. Lett.* **113**, 046802 (2014).
- [22] J. Song and E. Prodan, AIII and BDI topological systems at strong disorder, *Phys. Rev. B* **89**, 224203 (2014).
- [23] $\text{Tr}\Gamma = 0$ prevents the divergence of $F_j(z)$ with $H = \Sigma_{\text{ac}}(z) = 0$.
- [24] In general, Gell-mann matrices cannot decompose into commutable and anticommutable parts.
- [25] A. Y. Kitaev, Unpaired majorana fermions in quantum wires, *Physics-Uspokhi* **44**, 131 (2001).
- [26] A. Umerski, Closed-form solutions to surface green's functions, *Phys. Rev. B* **55**, 5266 (1997).
- [27] Åke Björck and G. H. Golub, Eigenproblems for matrices associated with periodic boundary conditions, *SIAM Rev.* **19**, 5 (1977).
- [28] H. Katsura and T. Koma, The noncommutative index theorem and the periodic table for disordered topological insulators and superconductors, *Journal of Mathematical Physics* **59**, 031903 (2018).
- [29] R. M. Lutchyn, J. D. Sau, and S. Das Sarma, Majorana fermions and a topological phase transition in semiconductor-superconductor heterostructures, *Phys. Rev. Lett.* **105**, 077001 (2010).
- [30] Y. Oreg, G. Refael, and F. von Oppen, Helical liquids and majorana bound states in quantum wires, *Phys. Rev. Lett.* **105**, 177002 (2010).
- [31] V. Mourik, K. Zuo, S. M. Frolov, S. R. Plissard, E. P. A. M. Bakkers, and L. P. Kouwenhoven, Signatures of majorana fermions in hybrid superconductor-semiconductor nanowire devices, *Science* **336**, 1003 (2012).
- [32] S. Rex and A. Sudbø, Tilting of the magnetic field in majorana nanowires: Critical angle and zero-energy differential conductance, *Phys. Rev. B* **90**, 115429 (2014).
- [33] W. P. Su, J. R. Schrieffer, and A. J. Heeger, Solitons in polyacetylene, *Phys. Rev. Lett.* **42**, 1698 (1979).
- [34] W. P. Su, J. R. Schrieffer, and A. J. Heeger, Soliton excitations in polyacetylene, *Phys. Rev. B* **22**, 2099 (1980).
- [35] S. Tamura, S. Nakosai, A. M. Black-Schaffer, Y. Tanaka, and J. Cayao, Bulk odd-frequency pairing in the superconducting su-schrieffer-heeger model, *Phys. Rev. B* **101**, 214507 (2020).
- [36] M. Scollon and M. P. Kennett, Persistence of chirality in the su-schrieffer-heeger model in the presence of on-site disorder, *Phys. Rev. B* **101**, 144204 (2020).
- [37] G. Tatara, H. Kohno, and J. Shibata, Microscopic approach to current-driven domain wall dynamics, *Physics Reports* **468**, 213 (2008).
- [38] D. Vanderbilt, *Berry Phases in Electronic Structure Theory: Electric Polarization, Orbital Magnetization and Topological Insulators* (Cambridge University Press, Cambridge, 2018).
- [39] L. Lin, Y. Ke, and C. Lee, Real-space representation of winding number for one-dimensional chiral-symmetric topological insulator (2021), arXiv:2101.08546.

Appendix A: List of notation

In the table I, we show the list of notation given in the main text.

TABLE I. List of notation. OBC and PBC indicate the open and periodic boundary condition, respectively. We also list the size of a space where the trace (Tr) and chiral operator (Γ) act.

$\Psi, H, G(z), F(z), \bar{G}(z), \bar{F}(z)$	OBC
$F_j(z), \Sigma_c(z), \Sigma_{ac}(z)$	
$\psi, h(k), h, g(k, z), g(z), w(z),$	PBC
$\bar{g}(k, z), \bar{g}(z), \bar{w}(z), \sigma_c(z), \sigma_{ac}(z)$	
Tr, Γ	$m \times m$ space
$\bar{\text{Tr}}, \bar{\Gamma}$	$mN_{\text{unit}} \times mN_{\text{unit}}$ space

Appendix B: Proof of generalized SBBC

In this appendix, most of the quantities denoted by upper-case (lower-case) letters are defined in the open (periodic) boundary condition system and we use a bit different notation from the main text.

We follow the same procedure as in the Daido and Yanase's paper [12] to prove Eq. (20):

$$\bar{\mathcal{F}} = \bar{\mathfrak{w}} \quad (\text{B1})$$

with

$$\bar{\mathcal{F}} = \frac{1}{N_{\text{diff}}} \sum_{j=N_i}^{N_f} \mathcal{F}_j, \quad (\text{B2})$$

$$\mathcal{F}_j = \sum_{l=1}^j \bar{\text{Tr}}[\mathcal{N}_l D_c \bar{\Gamma} \bar{\mathcal{G}}], \quad (\text{B3})$$

$$\bar{\mathfrak{w}} = \frac{1}{2iN_{\text{unit}}} \bar{\text{Tr}}\{\bar{\Gamma} \bar{\mathfrak{g}} i[\bar{\mathfrak{g}}^{-1}, \bar{x}]\}, \quad (\text{B4})$$

with $N_{\text{diff}} = N_i - N_f + 1$ and \bar{x} given by Eq. (12). Here $\bar{\mathcal{F}}$ is defined in the system with the open boundary condition at the both edges, $\bar{\mathfrak{w}}$ is defined in the system with the periodic boundary condition. Here, $\bar{\mathcal{G}}$ and $\bar{\mathfrak{g}}$ are given by

$$\bar{\mathcal{G}} = [D_c + D_{ac}]^{-1}, \quad (\text{B5})$$

$$\bar{\mathfrak{g}} = [d_c + d_{ac}]^{-1}, \quad (\text{B6})$$

where $D_{c,ac}$ and $d_{c,ac}$ satisfy following relations:

$$0 = [\bar{\Gamma}, D_c] = \{\bar{\Gamma}, D_{ac}\}, \quad (\text{B7})$$

$$0 = [\bar{\Gamma}, d_c] = \{\bar{\Gamma}, d_{ac}\}. \quad (\text{B8})$$

Here we assume $D_c + D_{ac}$, D_c , $d_c + d_{ac}$ and d_c are regular matrices and its matrix elements are short range in a real space basis. For example, Eq. (15) with $z\bar{F}(z) = \bar{\mathcal{F}}$ and $\bar{w}(z) = \bar{\mathfrak{w}}$ is reproduced by setting

$$D_c = z - \Sigma_c(z), \quad (\text{B9})$$

$$D_{ac} = -H - \Sigma_{ac}(z). \quad (\text{B10})$$

Then Eq. (B3) can be written as

$$\begin{aligned} \mathcal{F}_j &= \sum_{l=1}^j \bar{\text{Tr}}\left\{\mathcal{N}_l D_c \bar{\Gamma} [D_c + D_{ac}]^{-1}\right\} \\ &= \sum_{l=1}^j \bar{\text{Tr}}\left\{\mathcal{N}_l \bar{\Gamma} [1 + D_{ac} D_c^{-1}]^{-1}\right\}. \end{aligned} \quad (\text{B11})$$

$[1 + D_{ac} D_c^{-1}]^{-1}$ in Eq. (B11) is similar to $(z - H)^{-1}$ where H is replaced by $D_{ac} D_c^{-1}$. Recognizing this correspondence and then following the Daido and Yanase's paper [12], we can prove the generalized SBBC.

Appendix C: $\rho_A(E) - \rho_B(E)$ for SSH model

Analytical expression of the difference of the DOS for the SSH model is given by

$$\rho_A(E) - \rho_B(E) = -\frac{1}{\pi} \text{Im}[w(E + i\eta)/(E + i\eta)], \quad (\text{C1})$$

$$\begin{aligned} &w(E + i\eta) \\ &= \frac{1}{2} \left[1 - \frac{[t_1^2 - t_2^2 - (E - i\eta)^2](-1)^{f(t_1, t_2, E + i\eta)}}{\sqrt{[t_1^2 + t_2^2 - (E + i\eta)^2]^2 - (2t_1 t_2)^2}} \right], \end{aligned} \quad (\text{C2})$$

with

$$f(t_1, t_2, z) = \max\{n \in \mathbb{Z} \mid n \leq \tilde{f}(t_1, t_2, z)\}, \quad (\text{C3})$$

$$\begin{aligned} \tilde{f}(t_1, t_2, z) &= \frac{1}{2\pi} (\pi - \arg[t_1 - t_2 - z] + \arg[t_1 + t_2 - z] \\ &\quad - \arg[t_1 - t_2 + z] + \arg[t_1 + t_2 + z]). \end{aligned} \quad (\text{C4})$$